

CHEMICAL AND THERMODYNAMIC CONSTRAINTS ON THE THERMAL EVOLUTION OF EUCRITES. J. S. Gorce^{1,2}, D. W. Mittlefehldt², J. I. Simon², ¹Lunar and Planetary Institute, USRA, 3600 Bay Area Blvd., Houston TX 77058, USA (jgorce@lpi.usra.edu). ²Astromaterials Research and Exploration Sciences, NASA Johnson Space Center, Houston, TX 77058, USA.

Introduction: Vesta is the only differentiated asteroid with a nearly intact crust, making it the candidate for studying early planetary differentiation. It is commonly thought that the howardite, eucrite, and diogenite (HED) clan of meteorites derive from Vesta, and thus the study of HEDs is important for understanding the evolution of primitive bodies in the early solar system [1]. Of particular interest are the unusual trace element abundances in Stannern group eucrites, which have been interpreted as partial melting and melt contamination events that occurred on the parent body during thermal metamorphism [2]. However, some samples that contain evidence of high temperature metamorphism, such as Elephant Moraine (EET) 90020, have anomalous REE patterns that have been interpreted multiple ways. For example [3] concluded that the loss of small degrees of partial melt depleted the sample in LREEs while [4] concluded that subsolidus diffusion better explained why depletion of only some highly incompatible elements is observed. The heterogeneous nature of this sample makes reconstructing its petrologic history challenging.

Here, we conduct further petrographic and chemical studies on polished thin sections of EET 90020 and compare results to previous studies [3-5]. Additionally, we combine chemical analyses with thermodynamic models in order to refine the constraints on the post-crystallization thermal history of EET 90020. We additionally include studies of Graves Nunataks (GRA) 98098, which also contains evidence of high temperature metamorphism and anomalous geochemical signatures, as well as evidence of solid state diffusion at lower temperatures [6].

Sample description: EET 90020 is an unbrecciated, non-cumulate eucrite. We observe three distinctive textural domains: (i) coarse-grained, granoblastic plagioclase and pyroxene; (ii) medium-grained pyroxene with curved boundaries that are enveloped by rounded plagioclase; and (iii) fine-grained domains where interstitial space between plagioclase is filled by a silica phase. Plagioclase crystals are typically unzoned and calcic in composition (An_{86-92}). Pyroxenes have low-Ca hosts with average compositions of $Wo_{3.5}En_{33.7}Fs_{62.8}$ and high-Ca lamellae with average compositions of $Wo_{40.9}En_{28.1}Fs_{31.0}$. These observations are consistent with previous studies [3].

GRA 98098 is an unbrecciated, non-cumulate eucrite. Pyroxene and plagioclase vary in size, and form and ophitic to sub-ophitic texture. Pyroxene grains are larger than plagioclase grains (1 mm versus <0.5 mm), and exhibit exsolution lamellae of high-Ca augite (average $Wo_{38}En_{29}Fs_{33}$) in a low-Ca pigeonite host (average $Wo_{4.5}En_{36}Fs_{59.5}$). Lamellae are 10-15 μm thick. Plagioclase is Ca-rich (An_{87-91}). However, some plagioclase rims have Na-rich compositions (An_{75}). The sample also contains tabular laths of silica.

Thermodynamic modeling: Modeling was done using the thermodynamic software package *Perple_X*, which calculates mineral phase equilibria over a range of conditions using a Gibbs free energy minimization approach [7]. Calculations considered the components SiO_2 , TiO_2 , Al_2O_3 , Cr_2O_3 , FeO , CaO , MgO , MnO , Na_2O , and K_2O for a typical basaltic eucrite composition. Thermodynamic properties were used to constrain endmember phase stabilities [8-9]. Activity models for determining mixing between solid solution phases included a ternary feldspar model [10] a high temperature pyroxene that allows for Si-Al mixing on tetrahedral sites [11], and a melt model that has been calibrated to calculate partial melts of metabasic protoliths [11]. Isobaric models were computed at 1 bar to mimic conditions near Vesta's surface. For most models, oxygen fugacity was set at $\Delta IW-1$. However, several model iterations considered other f_{O_2} (e.g. $\Delta IW-2$, ΔIW) conditions to test the robustness of results.

Three different thermodynamic model types were used to study the thermal evolution of EET 90020 and GRA 98098. Isobaric thermal paths (Fig. 1) predicted crystallization and melting sequences and solid-state phase changes along a thermal profile for a fixed bulk rock composition. Isochemical Pressure-Temperature ($P-T$) phase diagrams further refined the temperature of metamorphism and attempted to constrain the depth of metamorphism. Temperature-Composition ($T-X$) phase diagrams assessed how heterogeneities in bulk rock composition affect phase stabilities and explored how contamination of eucrites via crustal partial melts might affect stable mineral assemblages.

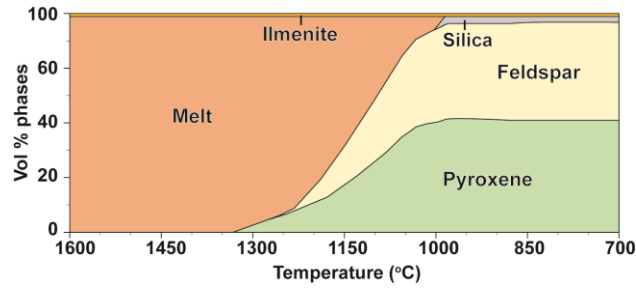


Figure 1: Isobaric thermal path for a basaltic eucrite composition that predicts the stable phases and abundances during cooling. Compositional data for individual phases are extracted from the model.

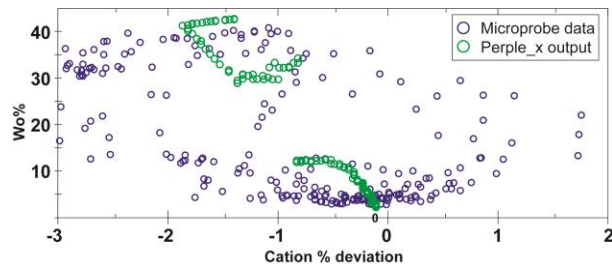


Figure 2: Plot of Wo% and cation % deviation in pyroxene analyses (blue) in comparison with the thermodynamically stable pyroxene compositions predicted for eucrites from solidus temperatures down to 700°C.

Discussion: Isobaric heating paths reasonably predict phase changes, abundances, and composition during cooling for eucrite compositions (Fig. 1) and fall within the range of measured compositional data (Fig. 2). Small partial melt fractions would produce silica rich melts that increase in FeO as temperature increases.

Preliminary P - T phase diagrams for GRA 98098 suggest that low-Ca pyroxene hosts equilibrated at temperatures from 750-900°C (Fig. 3a), which overlap with results from previous studies on EET 90020 that conclude that thermal metamorphism reached temperatures of 800-1000°C during longer duration thermal events and temperatures >1100°C for short duration thermal events [3, 5]. High-Ca exsolution lamellae do not exhibit overlap in pyroxene endmember components (Fig. 3b), and we tentatively suggest that this implies that the system did not achieve chemical equilibrium during the formation of high-Ca lamellae. Furthermore, the lower Ca content of augite in GRA 98098 ($Wo_{\sim 38}$) compared to EET 90020 ($Wo_{\sim 41}$) indicates a higher T of formation for the former.

Preliminary T - X diagrams suggest that the degree and composition of partial melts is influenced by the Mg # of the starting material.

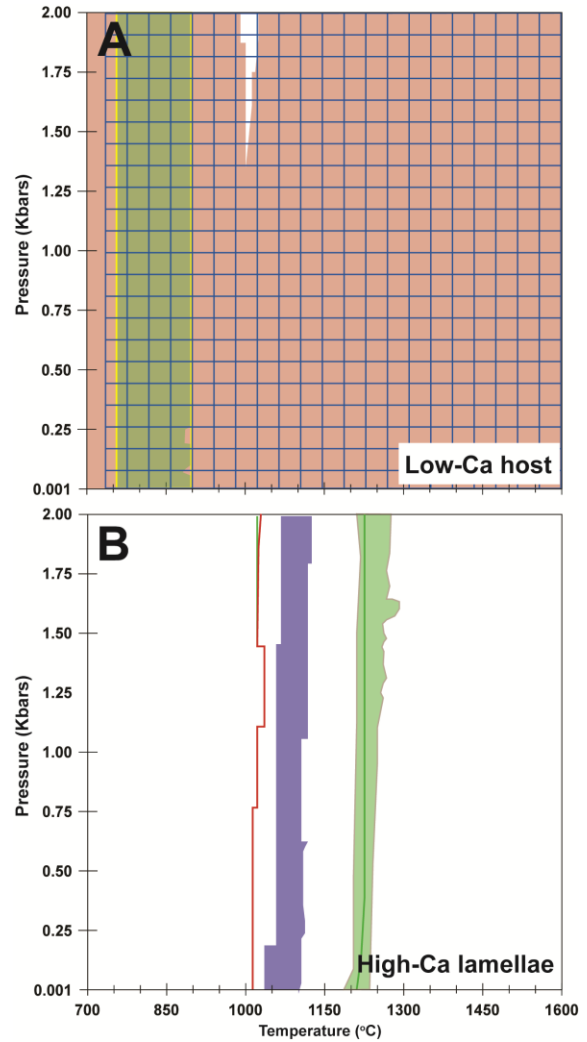


Figure 3: P - T phase diagrams that predict thermodynamically stable pyroxene compositions for GRA 98098. A) Overlap between Wo% (blue hatching), En% (red) and Fs% (green) fields represent the range of pressure and temperature conditions in which measured low-Ca host compositions are stable (yellow box). B) Stability fields of Wo%, En%, and Fs% for high-Ca lamellae do not overlap (colored as in A).

References: [1] Mittlefehldt D. W. (2015) *CdE-G*, 75, 155-183. [2] Barrat J. A. (2007) *GCA*, 71, 4108-4124. [3] Yamaguchi A. et al., (2001) *GCA*, 65, 3577-3599. [4] Mittlefehldt D. W. & Lindstrom M. M. (2003) *GCA*, 67, 1911. [5] Yamaguchi A. et al., (2009) *GCA*, 73, 7162-7182. [6] Mittlefehldt D. W. & Lee M. T. (2001) 64th MetSoc, A#5417. [7] Connolly J. A. D. (2005) *EPSL*, 236, 524-541. [8] Holland T. J. B. & Powell R. (1998) *JMG*, 16, 309-343. [9] Holland T. J. B. & Powell R. (2011) *JMG*, 29, 333-383. [10] Fuhrman M. L. & Lindsley D. H. (1988) *AM*, 73, 201-215. [11] Green E. C. R. et al. (2016) *JMG*, 34, 845-869.